J Exp Biol Advance Online Articles. First posted online on 8 June 2015 as doi:10.1242/jeb.119966
Access the most recent version at http://jeb.biologists.org/lookup/doi/10.1242/jeb.119966

Support for the beam focusing hypothesis in the false killer whale

Kloepper, L.N., Buck, J.R., Smith, A.B., Supin, A. Ya., Gaudette, J.E. and Nachtigall, P.E.

Keywords: Biosonar, Odontocetes, Echolocation, Whale

Abstract

The odontocete sound production system is complex and composed of tissues, air sacs, and a fatty melon. Previous studies suggested that the emitted sonar beam might be actively focused, narrowing depending on target distance. In this study, we further tested this beam focusing hypothesis in a false killer whale. Using three linear arrays of hydrophones, we recorded the same emitted click at 2, 4 and 7 m distance and calculated the beamwidth, intensity, center frequency, and bandwidth as recorded on each array at every distance. If the whale did not focus her beam, acoustics predicts the intensity would decay with range as a function of spherical spreading and the angular beamwidth would remain constant. On the contrary, our results show that as the distance from the whale to the array increases, the beamwidth is narrower and the received click intensity is higher than that predicted by a spherical spreading function. Each of these measurements is consistent with the animal focusing its beam on a target at a given range. These results support the hypothesis that the false killer whale is "focusing" its sonar beam, producing a narrower and more intense signal than that predicted by spherical spreading.

Introduction

Odontocetes, or toothed whales, dolphins and porpoises, produce intense, directional, ultrasonic echolocation signals and use the information in the returning echoes to identify, localize, and track prey. Unlike most mammals that use the larynx for sound production, odontocetes have evolved an elaborate sound production mechanism in their nasal cavity. Air is pressurized in a bony cavity and pushed upwards across soft tissue structures called the phonic lips. As air passes across these lips, the lips hit each other, presumably causing the associated fatty bursae structures to vibrate, creating the echolocation pulses. These pulses reflect anteriorly off both the curvature of skull and associated posterior air sacs, and propagate through the melon before being transmitted to the water (Cranford et al., 1996).

The origin of the term "melon" may be traced back to Captain David Gray, Commander of the Whaling Steamer "Eclipse," who, in describing the anatomy of a Bottlenose whale (*Hyperoodon rostratus*) remarked "In the males, instead of oil there is a

solid lump of fat similar in shape to, and about twice the size of, a large water-melon (Gray and Flower, 1882)." The unique structure of the melon was further described by A. Ohlin who further remarked on the structure "...somewhat resembling the cells of a bee-hive. The rooms between the fibrous bands are filled with a clear thin-floating oil (Ohlin, 1893)." Since these early reports, we now have a better understanding of the structure and composition of the melon. The melon is ovoid in shape and located slightly right of the midline in the forehead (Heyning, 1989). The melon itself has both an outer core, composed of both acoustic fats and connective tissue, and an inner core, composed mainly of acoustic fats (Heyning, 1989; Litchfield and Greenberg, 1973; Mead, 1975; Norris and Harvey, 1974). The acoustic fats are composed primarily of wax esters, which are metabolically toxic to the animal. This toxicity reinforces the importance of the melon to odontocetes; despite representing a significant investment of energy, individuals maintain the structure of the melon during periods of starvation (Cranford et al., 1996; Koopman et al., 2003). This implies that the melon serves a crucial functional role for odontocetes. Within the melon, the lipids are distributed in such a manner that there is a variable topography of chemical properties and sound speeds, which together help collimate the sound anteriorly (Litchfield and Greenberg, 1973; Norris and Harvey, 1974). Surrounding the melon is a network of facial muscles (Cranford et al., 1996; Heyning, 1989; Huggenberger et al., 2009; Mead, 1975), which may change the size and/or shape of the melon and associated air sacs (Harper et al., 2008; Huggenberger et al., 2009).

The melon has been hypothesized to act as an acoustic lens, shaping and focusing the emitted sound beam (Evans and Prescott, 1962; Norris, 1964). Some studies have attempted to investigate this hypothesis with a modeling approach, and found that the melon does play a role in beam formation (Aroyan et al., 1992; Cranford et al., 2014). Limitations of the modeling studies include using tissue properties from post-mortem specimens (Aroyan et al., 1992) and ignoring any conformational changes to the melon produced either intentionally or coincidentally by the animal (Cranford et al., 1996). Recently this beam focusing hypothesis was empirically tested in a live animal during echolocation (Kloepper et al., 2012). The results from that study showed that the beam area changed with range in a manner that could not solely be predicted by changes in the center frequency. This suggested that active focusing might be playing a role in determining beamwidth, but due to the design of the experiment the focusing of the beam across distance could not be directly tested.

Sound commonly propagates in a divergent manner, with the same energy spreading over a larger surface area as it propagates away from the source. The simplest divergent

propagation is spherical spreading, where the acoustic energy is equally distributed across all azimuths and elevations. In this model, the pressure field amplitude decays with 1/r and the intensity decays as $1/r^2$ (where r is range from the source) to account for spreading the same energy over a larger surface area as the wavefront propagates away from the source. Many marine mammals transmit sound with a directional characteristic, where the pressure (and intensity) at certain azimuths and elevations is greater than at others. The far field pressure for directional propagation is modeled as a product of two terms: one term for the angular dependence and the other term represents the 1/r spreading (Au and Hastings, 2008; Kinsler et al., 2000; Urick, 1983). The beam pattern is the angular dependence term normalized for the maximum on-axis pressure at a given range. This directional propagation model predicts that the beam will have constant angular width but increasing beam area as the sound propagates away from the source. Consequently, the intensity, or energy per unit area, must decrease as the distance from the source increases. The 1/r spreading term in the pressure results in a $1/r^2$ decay in intensity, conserving energy as the constant width beam propagates to greater range.

The alternative to divergent propagation is convergent propagation, or focusing. In this case, the wavefronts converge to interfere constructively. The location of this convergence is known as the focal range (FR). One method for creating convergent propagation is to cause the sound to propagate through a region of reduced sound speed, or increased index of refraction (Kinsler et al., 2000; Urick, 1983). Such a region acts as an acoustic lens, as illustrated in Fig. 1. Depending on the distance from the sound generator (SG) to the lens, and also the size, shape and sound speed of the lens, this acoustic lens can produce a beam that is still divergent (Fig. 1A), constant in area (Fig. 1B) or converging to a FR then diverging again beyond the FR (Fig. 1C). A consequence of focused propagation as shown in both Figs. 1B and 1C is that the angular beam width decreases with increasing range from the animal (up to the FR in 1C), and the intensity pressure does not display the $1/r^2$ spreading behavior (or 1/r behavior in pressure). Instead the focusing results in intensity which increases closer to the FR (Fig. 1C) or remains constant (Fig. 1B) with range.

The propagation of sound through the head of a marine mammal is more complicated than the simple optical lens in Fig. 1. However, the underlying refraction mechanism and fundamental nature of acoustic propagation (divergent, convergent, or constant width) are the same. For the case of convergent propagation (1C), the distance from the SG (the phonic lips) to L (the melon) is fixed by anatomy. However, changing the shape of the melon will alter the propagation characteristics of the sonar beam, including the FR.

In this study, we tested whether the false killer whale uses an unfocused or a focused beam during echolocation. Specifically, we tested two hypotheses: first, does the whale focus its beam, and second, does the whale focus its beam adaptively (i.e. according to target distance and condition)? While the whale echolocated on targets at three distances (2, 4 and 7 m), the sonar beam was recorded with three linear arrays at the three target distances. The intensity and beamwidth was calculated at each distance and compared to the divergent propagation model. When the target was located at distances of 4 m or greater, the echolocation beam width narrowed with distance, and the pressure was greater than predicted by 1/r spreading. During target absent trials, the whale adapted its beam similar to the farthest expected distance. These results support the hypothesis that the false killer whale focuses its sonar beam according to target distance, producing a convergent beam with an adaptable FR.

Results

Recording signals along the beam axis

To determine the near-to-far field transition, the sound pressure level (SPL) was recorded along the beam axis from 0.5 to 7 m while the whale performed a target detection task with the target located at 8 m. At distances less than 2 m, the relative SPL (SPL at a distance R subtracted from the SPL at 2 m) deviated from the spherical spreading function, but at distances greater than 2 m the relative SPL approximated a spherical spreading function (Fig. 3). Therefore, when a target is located at 8 m the acoustic far field for the subject begins at a distance between 1.5 and 2 m away from the blowhole, and all three linear array distances are located in the far field of the whale.

Recording the sonar beam at three distances

To test the first hypothesis that the whale uses a focused convergent beam, and not a constant width divergent beam, we measured the beamwidth at each of the three arrays. We performed the multivariate T^2 test for all three target ranges (2, 4, and 7 m) and for both target conditions (present and absent). For each of the six tests, the width of the known constant width beam was the average beamwidth over all trials and measurement arrays for that target range and condition. This choice for the known constant beamwidth is the most conservative. Any other choice for constant beam width would bias the tests towards significance. For the target present condition, the focusing was significant for the 2m target [$T^2(69,3) = 0.2582$, $p < 0.01$], 4m target [$T^2(100,3) = 0.4573$, $p < 0.001$] and 7m target

[$T^2(105,3) = 0.4652$, $p < 0.001$]. For the target absent condition, the focusing was significant at $p<0.001$ for all three target ranges: 2m [$T^2(135,3) = 0.2846$], 4m [$T^2(84,3) = 0.4625$] and 7m [$T^2(125,3) = 0.3389$].

To test the second hypothesis that the whale not only focuses its sonar beam, but adapts the focus to target distance and condition, we used a multivariate ANOVA (MANOVA) to determine the effect of target distance, target presence, and click number on beamwidth, normalized voltage and center frequency. For beamwidth, the multivariate result was significant for target distance [Pillai's Trace = 0.171, $F(6, 570) = 8.867$, $p < 0.001$], but not significant for target presence [Pillai's Trace = 0.011, $F(3, 284) = 1.082$, $p = 0.357$] or click [Pillai's Trace = 0.060, $F(15, 858) = 0.06$, $p = 0.293$]. The interaction of target distance and target presence was significant [Pillai's Trace = 0.236, $F(6, 570) = 12.68$, $p < 0.001$]. For most of the target conditions, beamwidth narrowed with increasing array distance (Fig. 4). For normalized voltage, the multivariate result was significant for target distance [Pillai's Trace = 0.137, $F(6, 570) = 6.982$, $p < 0.001$], target presence [Pillai's Trace = 0.086, $F(3, 284) = 8.962$, $p < 0.001$], the interaction of target distance and target presence [Pillai's Trace = 0.155, $F(6, 570) = 7.970$, $p < 0.001$], and click [Pillai's Trace = 0.138, $F(15, 858) = 2.763$, $p < 0.001$]. For most of the target conditions, the normalized voltage increased with increasing array distance (Fig. 5). For center frequency, the multivariate result was significant for target distance [Pillai's Trace = 0.112 $F(6, 570) = 5.651$, $p < 0.001$], target presence [Pillai's Trace = 0.061, $F(3, 284) = 6.170$, $p < 0.001$], the interaction of target presence and target distance [Pillai's Trace = 0.243, $F(6, 570) = 13.112$ $p < 0.001$], but not significant for click [Pillai's Trace = 0.075, $F(15,858) = 1.458$, $p = 0.114$]. For most target conditions, there was a slight decrease in center frequency with increasing array distance (Fig. 6).

Discussion

Our results support the hypothesis that the false killer whale focuses its echolocation beam onto a target. By recording the same echolocation click as it propagates through the water, we determined that the emitted beam of the false killer whale has a narrower beam and higher intensities at distance than would be predicted by spreading losses alone. For the target conditions where we see a consistent beam narrowing with distance (7 m present and all absent conditions), the angular beamwidth decreased by an average of 13.92% and source levels increased by an average of 1.73 dB between the 2 m and 7 m array.

Beamwidth, intensity, and center frequency are linked, such that higher intensity signals have higher center frequencies and narrower beamwidths (Au et al., 1995; Kloepper et al., 2012).

If the focusing observed is caused by changes in the signal spectrum decreasing the center frequency with range, the beamwidths should increase at the more distant arrays, not decrease, since lower frequency signals have broader beamwidths. If the decreases in beamwidth and increases in normalized voltage were due to changes in the signal spectrum and center frequency as the click propagates out in range, the center frequencies across the arrays should increase for the target conditions. Instead, we measured a small (200-400 Hz) decrease in center frequency over the distance of the arrays (Fig. 6). This decrease may be caused by the preferential attenuation of the higher frequency portion of the signal with range, which would result in a decrease in the center frequency. Because lower frequency signals have wider main lobes, this decreasing trend in center frequency over array distance would predict the beamwidth increasing with distance. Instead, we observed a decrease in beamwidth over distance, which further supports the hypothesis that the whale is actively focusing its echolocation beam to decrease beamwidth.

To further explore the relationship of beamwidth and voltage with distance, we expanded our dataset to include all the clicks produced by the whale across all trials and sessions. We separated signals into categories for individual analysis. All echolocation clicks were classified by beamwidth according to the following criteria (Fig. 7A):

Type 1: $w(2\text{ m}) > w(4\text{ m}) > w(7\text{ m})$

Type 2: $w(2\text{ m}) \leq w(4\text{ m}) \leq w(7\text{ m})$

Type 3: $w(2\text{ m}) \leq w(4\text{ m})$, $w(2\text{ m}) \leq w(7\text{ m})$, $w(4\text{ m}) > w(7\text{ m})$

Type 4: $w(2\text{ m}) \leq w(4\text{ m})$, $w(2\text{ m}) > w(7\text{ m})$, $w(4\text{ m}) > w(7\text{ m})$

Type 5: $w(2\text{ m}) > w(4\text{ m})$, $w(2\text{ m}) > w(7\text{ m})$, $w(4\text{ m}) \leq w(7\text{ m})$

Type 6: $w(2\text{ m}) > w(4\text{ m})$, $w(2\text{ m}) \leq w(7\text{ m})$, $w(4\text{ m}) \leq w(7\text{ m})$

If the whale did not focus its beam, the beamwidth would be constant at all distances, and small noise perturbations and experimental errors would produce an equal distribution of beam types across all target conditions. If the animal did focus its beam we would expect two outcomes depending on the method of focusing: 1) If the whale consistently narrowed her beam with distance, or had a FR much larger than any of the target ranges, we would expect an equal distribution of Type 1 beams across all target condition. 2) If, however, she used a strategy of creating a FR according to target distance, as hypothesized by previous work (Kloepper et al., 2012), we would expect the beam to be narrowest at the target distance, and

the other array distances intermediary in size, as illustrated in Fig. 1 C. Thus, we would expect a higher proportion of Type 2 signals when the target is at the 2 m distance, a higher proportion of Type 5 or 6 signals when the target is at the 4 m distance, and a higher proportion of Type 1 signals when the target is at the 7 m distance. According to the distribution of pulse types according to target condition in Fig. 7B, it appears the animal is using both strategies for beam focusing. For the 7 m target present and target absent conditions at all distances, the whale overwhelmingly produces Type 1, or narrowing with distance, signals (Fig. 7B). These data are consistent with prior work indicating that when there is a target absent condition, odontocetes attend to the farthest expected target range (Kloepper et al., 2014). For the other target present distances, the whale produces some Type 1 signals, which suggests the whale is still searching at the farthest target range, but the most frequently produced pulse types are Type 3 and 4 for the 2 m distance target and type 5 for the 4 m target.

We may take a cue from optics to help explain these results. The ovoid melon of the odontocete forehead may be roughly modeled as a biconvex lens. These lenses are thicker in the center and thinner at the periphery, which causes a convergence of light, or a focal point (Sharma, 2006). This focusing results in a narrowing of the beam to a certain region, then an expanding of the beam beyond that FR. Changing the curvature or thickness of this lens can cause the FR to move closer to or farther from the lens. In odontocetes, changes in the curvature of the melon could be accomplished by manipulating the network of muscles that surround the melon (Mead, 1975).

The results for the 4 and 7 m target support the idea that the whale is narrowing the beam onto the target, but the results for the 2 m target do not. Particularly perplexing is that, for the measurements with the target at 2 m, the beam is narrowest at 2 m, widens at 4 m, and then narrows again at 7 m. There are several possible factors that might be contributing to these results. These include physical interactions in the near field, and biological limitations of the whale's focusing mechanism.

The acoustic near field is the region close to the source where the pressure field experiences complicated constructive and destructive interference patterns due to the sound radiating from different elements of the source. In the near field, the acoustic pressure is not well described by product of a range term and an angular term as it is in the far field (Foote, 2014; Urick, 1983). As a result, in the near field there is no clearly defined beamwidth, and the intensity of the sound does not obey 1/r spreading seen in the far field. Instead, the acoustic intensity in the near field varies rapidly as even small changes in frequency or

distance can move from constructive to destructive interference. We previously determined the near-to-far field transition for the animal to occur between 1.5 and 2 m when the target is located at 8 m distance (Fig. 3). If the animal were changing the shape of its melon depending on target distance, deformations in the melon would change the effective size of the transducer, which would also change the near-to-far field transition distance. Because our original near-to-far field region of 1.5 to 2 m was determined from a target distance of 8 m, we cannot rule out that the 2 m array is within the near field of the whale when the whale is echolocating on a target at 2 m.

The likelihood of the 2 m array being located in the near field for the 2 m target condition is further supported by a comparison of center frequency for the click types. For the Type 1 signals, which are presumably produced when the near-to-far field transition is greater than 2 m, there is no significant difference of center frequency between the clicks recorded on the 2 and 4 m arrays. For the Type 3 and Type 4 signals, however, there is a significant difference of center frequency between the clicks recorded on the 2 and 4 m arrays (Type 3 [$t(98) = 3.0861$, $p = 0.0026$] ; Type 4 [$t(96) = 3.0551$, $p = 0.0029$]), with a higher center frequency recorded on the 2 m hydrophone array compared to the 4 m array. Because frequency and beamwidth are inherently related (Au et al., 1995), this rise in frequency would be consistent with a narrowing of beam and may reflect interference patterns from being in the near field. Furthermore, since intensity and frequency of echolocation signals are related (Au et al., 1995; Kloepper et al., 2010a), if we were in the acoustic far field we would expect to find an associated significant difference in voltage between the 2 and 4 m arrays for the Type 3 and Type 4 signals. The fact that there is no significant difference ($p = 0.7332$ and $p = 0.7561$) is further evidence that we may be operating in the acoustic near field for the 2 m array, which would explain the anomalous beam results.

A second explanation for the results at the 2 m distance might be due to practical limitations of the focusing mechanism. If the focusing is caused by muscular deformation of the melon, there may be a physical limitation for a minimum FR. Focal ranges are reduced by increasing the curvature of the lens (Sharma, 2006), or equivalently reducing the radius of curvature. If there is a maximum curvature possible for the melon due to anatomical limitations, this would impose a minimum FR for the transmitted sonar waveform. Many odontocete species produce low amplitude, high-repetition clicks (termed "buzzes") when prey are within one body length (DeRuiter et al., 2009; Johnson et al., 2004; Verfuss et al., 2009; Wisniewska et al., 2014). These buzzes are distinctly different than the clicks made when prey are at greater distances, and their rapid production rate may eliminate any need for

focusing. When prey are at such close distances and echolocation clicks are produced at a rapid rate, there may be no advantage gained in focusing at a close range.

Using a focused echolocation beam has important ecological functions for odontocetes. By using internal structures to narrow the sound beam, the animal increases the intensity of the signal impinging on a target, which results in a louder returning echo. Changing the FR according to the target distance means the animal adapts its signal to ensure the returning echo, regardless of target distance, is as loud as possible, which may help in species that discriminate between species or forage on prey with weak echoes (Au et al., 2009; Kang et al., 2005). Additionally, the surface temperatures of seawater can vary as much as 20 degrees C over *Pseudorca*'s range, with a consequent change in soundspeed of 90 m/s (Kinsler et al., 2000). This temperature driven sound speed change can change the index of refraction significantly for the water surrounding the animal throughout the year. From this point of view, the animals are likely to alter their melon to compensate for the changes in refraction due to seasonal temperature variations. If the melon were fixed in shape, the animal would suffer from a sonar beam that widened and narrowed in angle and moved its FR nearer and further as the water temperature varied annually.

The results from this study further raise an interesting question of what is the "default," or relaxed, state for an echolocating animal that focuses its sound beam. Based on the results from the target absent condition, that is, the whale focuses its sonar to the farthest expected target distance, one hypothesis is that the natural state is to focus the beam at long range. Intuitively this makes ecological sense since the whale will likely first detect an object at far range, then track and discriminate as the animal comes closer to the object. If this is indeed the strategy used by echolocating odontocetes, it suggests there is some cost associated with focusing its sonar beam.

Due to the similarity of sound producing structures across all odontocetes (Cranford et al., 1996), this sonar focusing strategy is likely not unique to the false killer whale. Instead, this may be an adaptive mechanism shared by all odontocetes. By using their unique sound focusing structures, odontocetes can optimize the energy impinging on a target, which would result in increased target detection, discrimination, and overall foraging success. Anatomical adaptation is common in many other animals and across sensory modalities (Estes, 1972; Forrester et al., 1996; Gao et al., 2011). Therefore, our proposed focusing mechanism for odontocetes is not unusual, but rather consistent with adaptive sensory behavior clearly demonstrated in many other animal species.

Materials and Methods

Animal and Environment

The experiments were conducted at the floating pen complex of the Marine Mammal Research Program of the Hawaii Institute of Marine Biology off Coconut Island, Kaneohe Bay, Oahu, Hawaii. The water surrounding the pens is approximately 22°C, 12 m deep, and has a thick mud substrate 1 m thick. The experimental subject was a female false killer whale [*Pseudorca crassidens* (Owen, 1846)] named Kina, measuring 3.96 m and weighing 540 kg. The exact age of Kina is unknown; she was brought to Hawaii as an adult in 1987 and is estimated to be over 30 years old.

Experimental procedure

The setup for the experiment is shown in Fig. 2A. The experiment utilized two separate pens: the experimental pen, a wire enclosure that measured 9.14 m wide, 12.19 m long, and 4.11 m deep and contained the whale; and the target pen, a wireless structure consisting of a floating dock that measured 6.10 m wide, 9.14 m long, and contained the echolocation targets and the recording equipment. During the experiment the subject would keep her body in the experimental pen but station her head through a hoop located 1 m below the surface of the water and ensonify the targets located in the target pen. An underwater camera (SCS Enterprises, Montebello, NY, USA) was used to monitor her hoop behavior. An acoustically opaque metal screen was located in front of the animal to prevent her from echolocating prematurely on the targets. An acoustically transparent, yet visually opaque polyethylene screen was placed in front of the acoustically opaque screen to ensure that the subject was not utilizing visual cues.

The subject was trained to detect the presence or absence of a hollow aluminum cylinder 12.7 cm long with an outer diameter of 37.85 mm and a wall thickness of 6.35 mm (the “standard” target from (Kloepper et al., 2010b)). When submerged, the cylinder filled with water. At the start of and between trials, the subject stationed horizontally at the water surface by placing the tip of her rostrum on a vertically placed pad on the side of the experimental pen near the trainer. When cued via a hand signal, the whale submerged and swam to the opposite side of the experimental pen, positioning herself into the underwater hoop up to her pectoral fins (thus positioning her head inside the target pen) and remained stationary for the trial. During the whale positioning time a target was placed into the water at 1 m depth for target-present “go” trials. At this point in time acoustic access to the target was blocked via the acoustically opaque screen and the animal produced bubbles that would help mask any potential target

splashing sounds. After the target was lowered into the water the acoustically opaque screen was moved to reveal the target. The subject ensonified the target pen and determined whether a target was present (a “go”) or absent (a “no-go”). If the target was present, the subject backed out of the hoop and touched a response paddle with her rostrum. If the target was absent (a “no-go”), the subject remained in the hoop until signaled out by the trainer. The subject was rewarded with fish for correct responses. Incorrect responses resulted in no fish reward. Thus, the general form of the procedure was a go/no go paradigm (Schusterman, 1980).

Determination of Near-to-Far Field

Echolocation signals were recorded in February 2011 using the same setup described above, with the animal detecting the presence or absence of a target located at 8 m. Eleven Reson 4013 (Reson, Slangerup, Denmark) hydrophones were positioned on a straight line from the head to the target at distances of 0.5, 0.75, 1.0, 1.25, 1.5, 2.0, 3.0, 4.0, 5.0, 6.0 and 7.0 m. The blowhole was taken as the zero point of the distance scale as a convenient mark located in close vicinity to the air sacks and melon, the head structures commonly considered as the sonar click generator and focusing device (Cranford et al., 1996). When the whale ensonified the target, each of her sonar clicks was recorded by these hydrophones. Each hydrophone was amplified by 20 dB using a custom built amplifier and sampled at a rate of 1 MHz using a NI DAQmx-PCI 6133 analog to digital (A/D) board (National Instruments, Austin, TX, USA) and custom LABVIEW software (National Instruments, Austin, TX, USA). Peak-to-peak voltage measurements were used to calculate the SPL for each hydrophone. 614 clicks from 30 click trains (trials) were recorded and averaged. The distance with which the near field transitioned to the far field was characterized as the distance where the acoustic pressure decreased by approximately the inverse of the distance (Au et al., 1978)

Recording the sonar beam at three distances

This experiment was conducted in February 2013. The experiment consisted of three sessions of 50 trials each. For each session, the target was presented at the same distance with 25 go trials and 25 absent trials. Thus, this was considered a "predictable" task for the animal (Kloepper et al., 2014). Echolocation signals were recorded with three linear arrays of 5 Reson 4013 hydrophones (Reson, Slangerup, Denmark) each positioned at 1 m depth and 2, 4 and 7 m distance (close, medium, and distant, Fig. 2C). Each array was composed of a polyvinyl chloride (PVC) framework in the shape of an upside-down American football field

goal and supported across the middle of the target pen by a large wooden support beam (Fig. 2D). Individual hydrophones were fixed in position with silicone adhesive to monofilament strung between the open ends of the PVC framework. Inter-sensor spacing of arrays was chosen to maintain consistent angular spacing with respect to the animal. The hydrophones were positioned 0.125 m, 0.25 m, and 0.4 m apart for the 2, 4, and 7 m distance arrays, respectively. This resulted in azimuthal spaced sampling of approximately 3.5 degrees between hydrophone elements (Fig. 2C). Each hydrophone occupied an independent channel and was amplified by 20 dB using a custom-built 16 channel pre-amplifier. Signals were digitized using two National Instruments DAQmx-PCI 6133 A/D boards (Austin, TX, USA) at a sample rate of 250 kHz.

Hydrophone Array Calibration

Prior to experimentation, the hydrophone arrays were ground truthed via a two-step procedure. First, each hydrophone was individually calibrated using a 45 kHz pure tone signal and a synthetic broadband click centered at 60 kHz, both using an custom ultrasonic broadband transducer (Whitlow Au, Marine Mammal Research Program) with a half power beamwidth of 14.5 degrees at 60 kHz. The receiving Reson 4013 hydrophones have a flat frequency response between 5 to 170 kHz. The receive voltage sensitivity (RVS) of each hydrophone varied by less than 1 dB re: 1V/μPa. Secondly, the hydrophone arrays were fixed in position and 30 synthetic clicks centered at 60 kHz were projected towards the center array elements. Time series data were recorded for all hydrophone elements on the three arrays using the same equipment as in the animal experiments. After resampling and computing the peak-to-peak click energy the measured beam pattern was interpolated using a cubic spline for each of the three arrays using MATLAB (Mathworks, Natick, MA, USA). Using the calibrated hydrophone RVS, data were then converted from voltage units to sound pressure level (dB SPL re: 1 μPa) and compensated for spherical spreading losses (dB SPL re: 1 μPa @ 1 m). Once the calibration was complete, the arrays remained in their fixed position for the duration of the experiment. The experiment was completed over a 36-hour time period of calm weather, which ensured no perturbations in the setup of our arrays.

Echolocation parameters

For each echolocation signal, the on-axis hydrophone was identified as the hydrophone of each array with the highest amplitude signal. Clicks in which the on-axis signal were on the peripheral hydrophones, or in which the on-axis hydrophone was not the

same for all three arrays were omitted from analysis. These criteria were used to ensure the -3 dB beam was correctly captured on all three arrays. This resulted in an analysis set of 1121 out of 1373 clicks for the three sessions. Due to variation in echolocation parameters across clicks within a trial (Kloepper et al., 2012, 2014), we chose five sequential clicks (clicks 5-10, which represent the peak emission within a pulse train) for further analysis. Using these clicks, the peak-to-peak voltage and center frequency (as defined in Au, 1993) were calculated for each click on each array distance (2, 4 and 7 m). The voltages of the on-axis signal were normalized relative to the expected transmission losses based on the calibration values; that is, if signals followed spherical spreading transmission losses we would expect a constant voltage across all three arrays. Thus, we are comparing a normalized voltage value. The center frequency values were compared to ensure that changes in the beamwidth or normalized voltage were not artifacts of frequency-dependent attenuation altering the signal spectrum during propagation. The-3dB beamwidth was calculated by cubically interpolating voltage values across the dimensions of each linear array and then determining the angular coordinates at which the echolocation signal crosses -3dB, or half power, the peak of the signal using a MATLAB program (see Fig. S1).

To test whether the beam is focused with convergent propagation, we analyzed the beamwidths measured at each array as multivariate data using multivariate T^2 statistics (Anderson, 2003**)** testing against a known hypothesis of constant beamwidth over distance. For each click recorded on axis, the beamwidths measured at the three arrays were combined into a multivariate measurement (3x1 vector). The most direct test that the beam is focused is a multivariate T^2 test against the known hypothesis that the angular beamwidth was constant across the three arrays (Anderson; 2003). This test is the multivariate analog of the basic T test for scalar data against a known mean value.

To test whether the beam is focused adaptively on target distance and presence, we used a multivariate analysis of variance (MANOVA) in SPSS (v. 22, IBM, Armonk, NY, USA) with target distance, target presence, and click number as fixed factors, and the three parameters (beamwidth, normalized voltage, and center frequency) at each of the three array distances as dependent multivariate observations.

Acknowledgements

This project would not have been possible without the efforts of the staff of the Marine Mammal Research Program, particularly trainers Marlee Breese, Christopher Quintos, and Stephanie Vlachos. This project was approved under permit from the National

Marine Fisheries Service to Paul E. Nachtigall. Work was approved under the University of Hawaii Institutional Animal Care Committee Protocol 93-005-15.

Funding

This project was funded by an Office of Naval Research grant N00014-12-1-02-12 awarded to PEN and the National Science Foundation Postdoctoral Research Fellowship in Biology DBI-120833 awarded to LNK.

Author contribution

All authors contributed significant and substantial contributions to the study.

Author competing interests

All authors declare no competing interests

List of abbreviations

FFT- Fast Fourier transform
NV- Normalized Voltage
PVC- Polyvinyl chloride
SPL- Sound pressure level
RVS- Receive voltage sensitivity

References

Anderson, T.W (2003). *An Introduction to Multivariate Statistical Analysis, Third Edition*, New York:Wiley.

Aroyan, J. L., Cranford, T. W., Kent, J. and Norris, K. S. (1992). Computer modeling of acoustic beam formation in *Delphinus delphis. J. Acoust. Soc. Am.* **92**, 2539–2545.

Au, W. and Hastings, M. C. (2008). *Principles of Marine Bioacoustics.* New York: Springer.

Au, W. W. L., Branstetter, B. K., Benoit-Bird, K. J. and Kastelein, R. A. (2009). Acoustic basis for fish prey discrimination by echolocating dolphins and porpoises. *J. Acoust. Soc. Am.* **126**, 460-467.

Au, W. W. L., Floyd, R. W. and Haun, J. E. (1978). Propagation of Atlantic bottlenose dolphin echolocation signals. *J. Acoust. Soc. Am.* **64**, 411-422.

Au, W. W. L., Pawloski, D., Nachtigall, P. E., Blonz, M. and Gisner, R. C. (1995). Echolocation signals and transmission beam pattern of a false killer whale (*Pseudorca crassidens*). *J. Acoust. Soc. Am.* **98**, 51-59.

Cranford, T. W., Trijoulet, V., Smith, C. R. and Krysl, P. (2014). Validation of a vibroacoustic finite element model using bottlenose dolphin simulations: the dolphin biosonar beam is focused in stages. *Bioacoustics* **23**, 161–194.

Cranford, T., Amundin, M. and Norris, K. S. (1996). Functional morphology and homology in the odontocete nasal complex: implications for sound generation. *J. Morph.* **228**, 223-285.

DeRuiter, S. L., Bahr, A., Blanchet, M. A., Hansen, S. F., Kristensen, J. H., Madsen, P. T., Tyack, P. L. and Wahlberg, M. (2009). Acoustic behaviour of echolocating porpoises during prey capture. *J. Exp. Biol.* **212**, 3100–3107.

Estes, R. (1972). The role of the vomeronasal organ in mammalian reproduction. *Mammalia* **36**, 315–341.

Evans, W. E. and Prescott, J. H. (1962). Observations of the sound production capabilities of the bottlenose porpoise: a study of whistles and clicks. *Zoologica* **47**, 121-128.

Foote, K. G. (2014). Discriminating between the nearfield and the farfield of acoustic transducers. *J. Acoust. Soc. Am.* **136**, 1511–1517.

Forrester, J., Dick, A., McMenamin, P. and Lee, W. (1996). *The Eye: Basic Sciences in Practice*. London: W.B. Saunders.

Gao, L., Balakrishnan, S., He, W., Yan, Z. and Müller, R. (2011). Ear deformations give bats a physical mechanism for fast adaptation of ultrasonic beam patterns. *Phys. Rev. Lett.* **107**, 214301.

Gray, D. and Flower, P. (1882). Notes on the characters and habits of the bottlenose whale (*Hyperoodon rostratus*). *Proc. Zool. Soc. Lond.* **50**, 726–731.

Harper, C. J., Mclellan, W. A., Rommel, S. A., Gay, D. M., Dillaman, R. M. and Pabst, D. A. (2008). Morphology of the melon and its tendinous connections to the facial muscles in bottlenose dolphins (*Tursiops truncatus*). *J. Morph.* **269**, 820–839.

Heyning, J. E. (1989). Comparative facial anatomy of beaked whales (Ziphiidae) and a systematic revision among the families of extant odontoceti. *Contr.Sci.* **405**, 1–64.

Huggenberger, S., Rauschmann, M. A., Vogl, T. J. and Oelschläger, H. H. A. (2009). functional morphology of the nasal complex in the harbor porpoise (*Phocoena phocoena* L.). *Anat. Rec.* **292**, 902–920.

Johnson, M., Madsen, P. T., Zimmer, W. M. X., de Soto, N. A. and Tyack, P. L. (2004). Beaked whales echolocate on prey. *Proc. R. Soc. B: Biol. Sci.* **271**, S383–S386.

Kang, D., Mukai, T., Iida, K., Hwang, D. and Myoung, J. (2005). The influence of tilt angle on the acoustic target strength of the Japanese common squid (*Todarodes pacificus*). *ICES J. Mar. Sci.* **62**, 779–789.

Kinsler, L. E., Frey, A. R., Coppens, A. B. and Sanders, J. V. (2000). *Fundamentals of Acoustics, Fourth Edition*. New York: John Wiley and Sons, Inc.

Kloepper, L. N., Nachtigall, P. E. and Breese, M. (2010a). Change in echolocation signals with hearing loss in a false killer whale (*Pseudorca crassidens*). *J. Acoust. Soc. Am.* **128**, 2233-2237.

Kloepper, L. N., Nachtigall, P. E., Gisiner, R. and Breese, M. (2010b). Decreased echolocation performance following high-frequency hearing loss in the false killer whale (*Pseudorca crassidens*). *J. Exp. Biol.* **213**, 3717–3722.

Kloepper, L. N., Nachtigall, P. E., Donahue, M. J. and Breese, M. (2012). Active echolocation beam focusing in the false killer whale, *Pseudorca crassidens*. *J. Exp. Biol.* **215**, 1306–1312.

Kloepper, L. N., Smith, A. B., Nachtigall, P. E., Buck, J. R., Simmons, J. A. and Pacini, A. F. (2014). Cognitive adaptation of sonar gain control in the bottlenose dolphin. *PLoS ONE* **9**, e105938.

Koopman, H. N., Iverson, S. J. and Read, A. J. (2003). High concentrations of isovaleric acid in the fats of odontocetes: variation and patterns of accumulation in blubber vs. stability in the melon. *J. Comp. Phys. B.* **173**, 247-261.

Litchfield, C. and Greenberg, A. J. (1973). Comparative lipid patterns in the melon fats of dolphins, porpoises and toothed whales. *Comparative Biochemistry and physiology, B*. **47**, 401-407.

Mead, J. G. (1975). Anatomy of the external nasal passages and facial complex in the delphinidae (Mammalia: Cetacea). *Smithsonian Contributions to Zoology* 1–80.

Norris, K. S. (1964). Some problems of echolocation in Cetaceans. *Marine Bio-acoustics* **2**, 317-336.

Norris, K. S. and Harvey, G W (1974). Sound transmission in the porpoise head. *J Acoust Soc Am* **56**, 659–664.

Ohlin, A. (1893). Some remarks on the bottlenose-whale (*Hyperoodon*). *Lunds Universitets Ars-skrift* **29**, 1–14.

Schusterman, R. J. (1980). Behavioral methodology in echolocation by marine mammals. In *Animal Sonar Systems* (eds. Busnel, R. G. and Fish, J. F.), pp. 14–41. New York: Plenum Press.

Sharma, K. K. (2006). *Optics: Principles and Applications*. Burlington, MA: Academic Press.

Urick, R. J. (1983). *Principles of Underwater Sound*. London: McGraw-Hill.

Verfuss, U. K., Miller, L. A., Pilz, P. K. D. and Schnitzler, H. U. (2009). Echolocation by two foraging harbour porpoises (*Phocoena phocoena*). *J Exp Biol* **212**, 823–834.

Wisniewska, D. M., Johnson, M., Nachtigall, P. E. and Madsen, P. T. (2014). Buzzing during biosonar-based interception of prey in the delphinids *Tursiops truncatus* and *Pseudorca crassidens*. *J Exp Biol* **217**, 4279–4282.

Figures

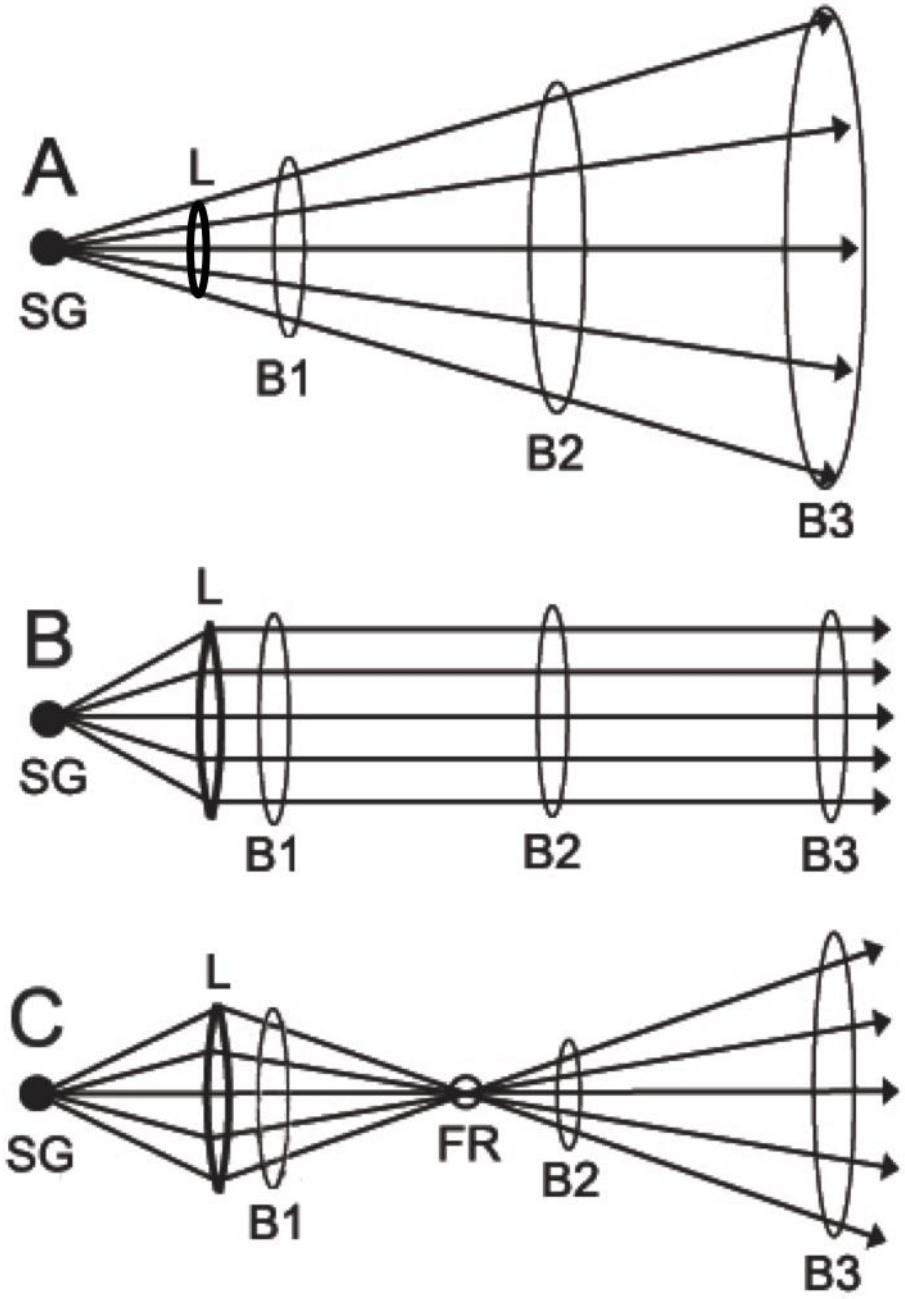

Figure 1: Different patterns of beam attenuation with distance. (A) Unfocused beam from a point source and ideal spherical spreading. Absolute beamwidth increases with distance, but angular beamwidth remains constant. (B) Ideally focused beam in which absolute beamwidth remains constant irrespective of distance, but angular beamwidth decreases with distance. (C) Convergently focused beam resulting in a focal region (FR) and variable angular beamwidth measurements. SG – sound generator, L – focusing lens, B1-B3-- variable beamwidths at different distances from the sound source.

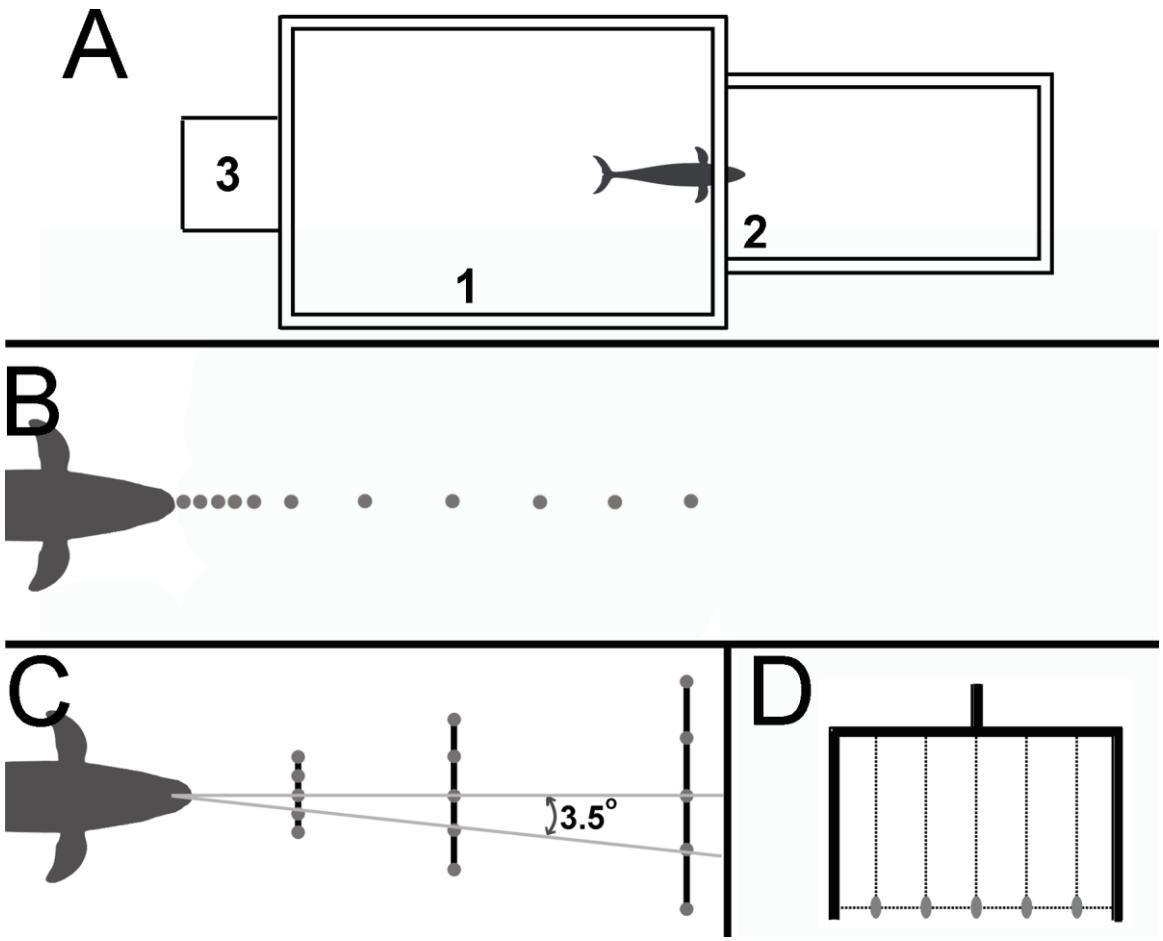

Figure 2: Experimental setup and array configurations. (A) Topside view of experimental pen (1), target pen (2), and trainer/equipment shack (3). (B) Topside view for near-to-far field transition determination with the phones located at 1 m depth and at distances of 0.5, 0.75, 1, 1.25, 1.5, 2, 3, 4, 5, 6 and 7 m from the blowhole. Hydrophone elements are indicated by the gray circles. (C) Topside view of linear arrays with the arrays located at 1 m depth and distances of 2, 4 and 7 m distance. Hydrophone elements are indicated by the gray circles, and the PVC framework is indicated by the black lines. The inter-sensor spacing was chosen to maintain angular spacing of approximately 3.5 degrees for each array. (D) Forward view of one array from the whale's perspective. Hydrophone elements are indicated by the gray oblongs, PVC framework is indicated by the black lines, and monofilament is indicated by the dashed lines.

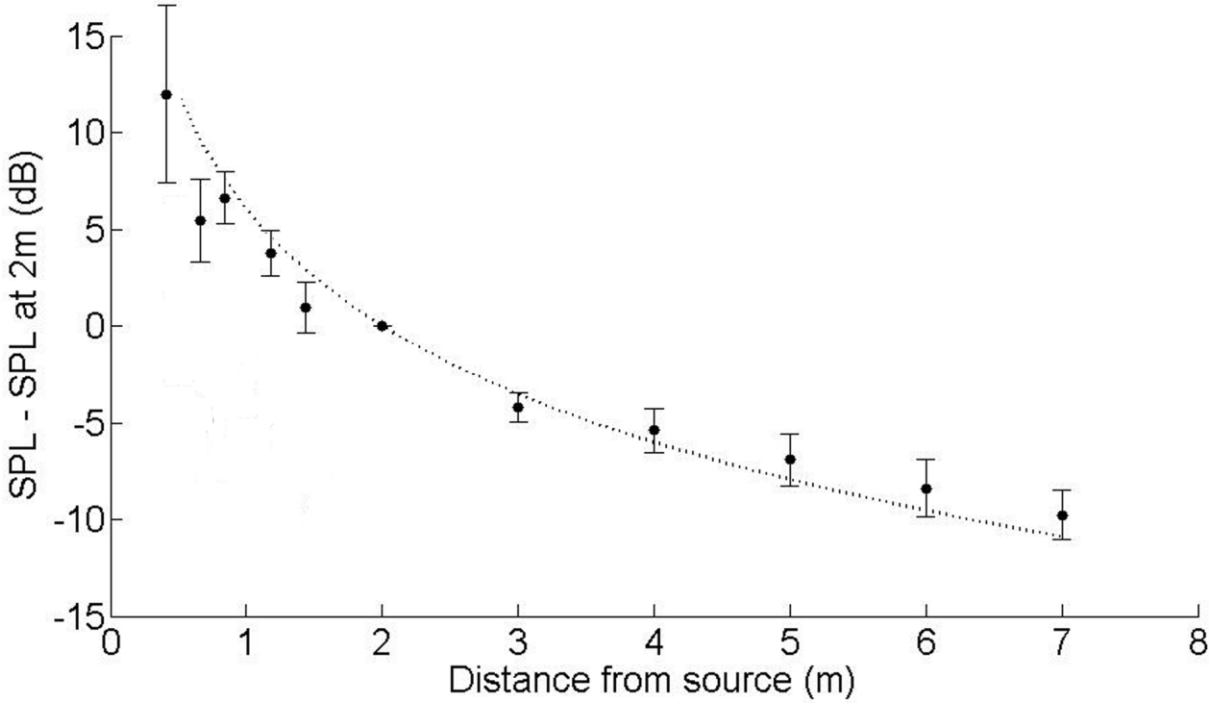

Figure 3. Recording signals along the beam axis (see Fig. 2B for experimental configuration). Relative sound pressure levels (in dB re: 1µPa) measured at a distance (in meters) from the sound source for 614 clicks from 30 click trains. The circles represent the mean difference between the SPL measured at a given distance (r) and the SPL measured at 2 m, and the bars represent the standard deviations of each point. The dashed curve represents the spherical spreading loss function of 1/r, with a reference at 2 m.

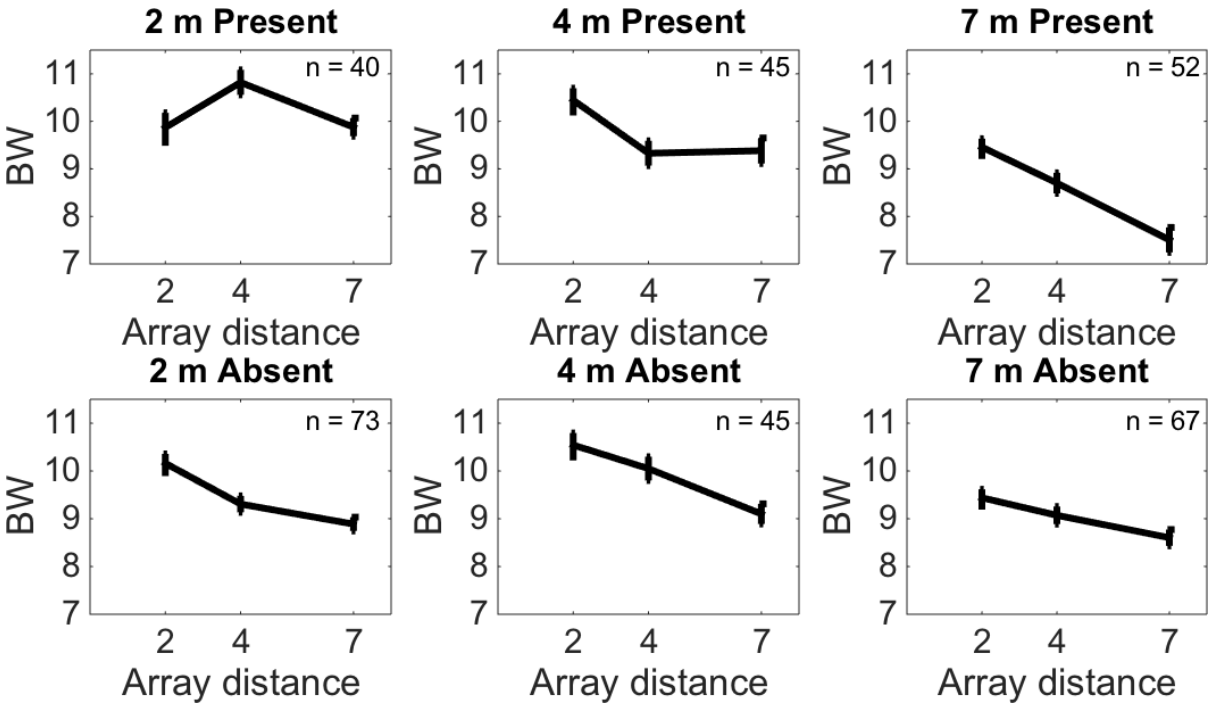

Figure 4: Mean and standard error in -3dB beamwidth (BW, in degrees) after cubic interpolation across the three recording arrays (distance, in m) for each target condition.

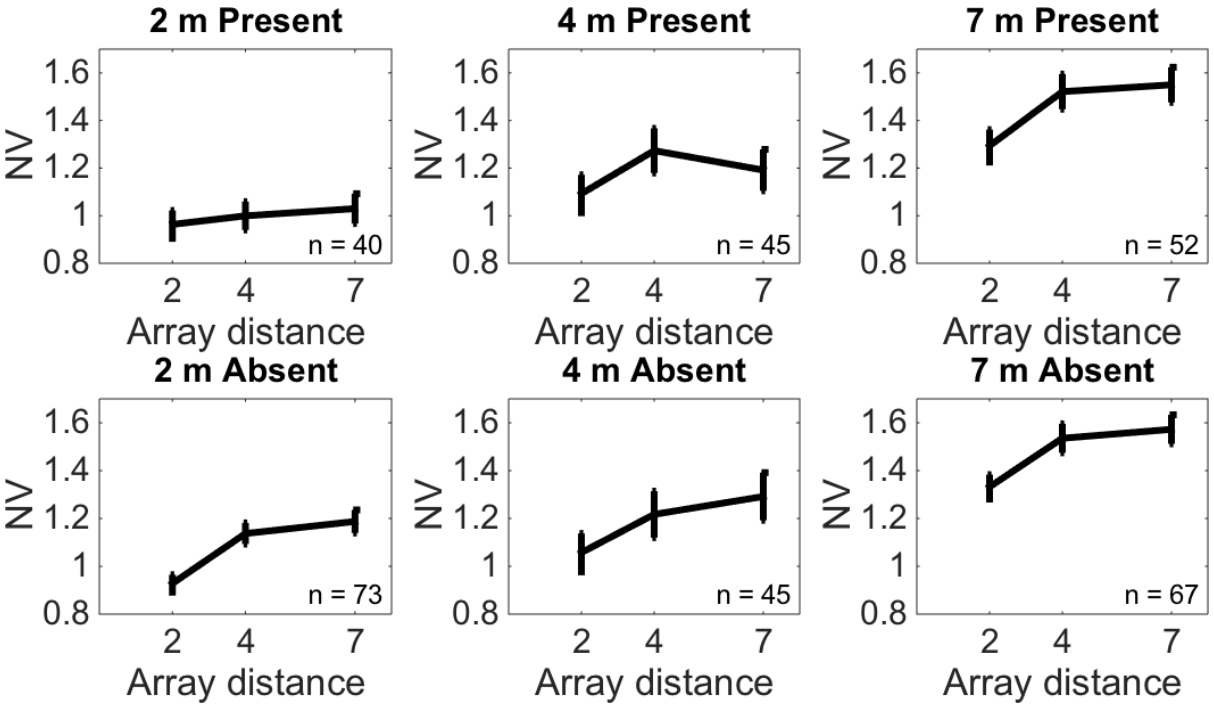

Figure 5: Mean and standard error in normalized voltage (NV) across the three recording arrays (distance, in m) for each target condition.

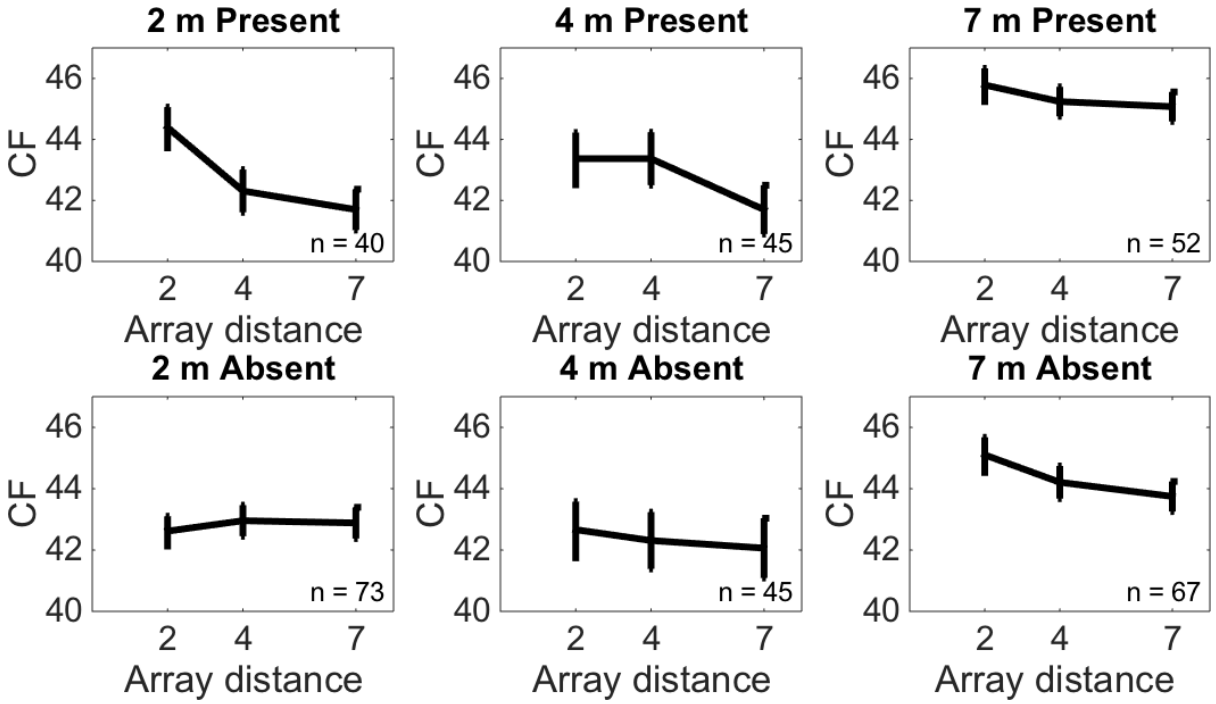

Figure 6: Mean and standard error in center frequency (CF, in kHz) after cubic interpolation across the three recording arrays (distance, in m) for each target condition.

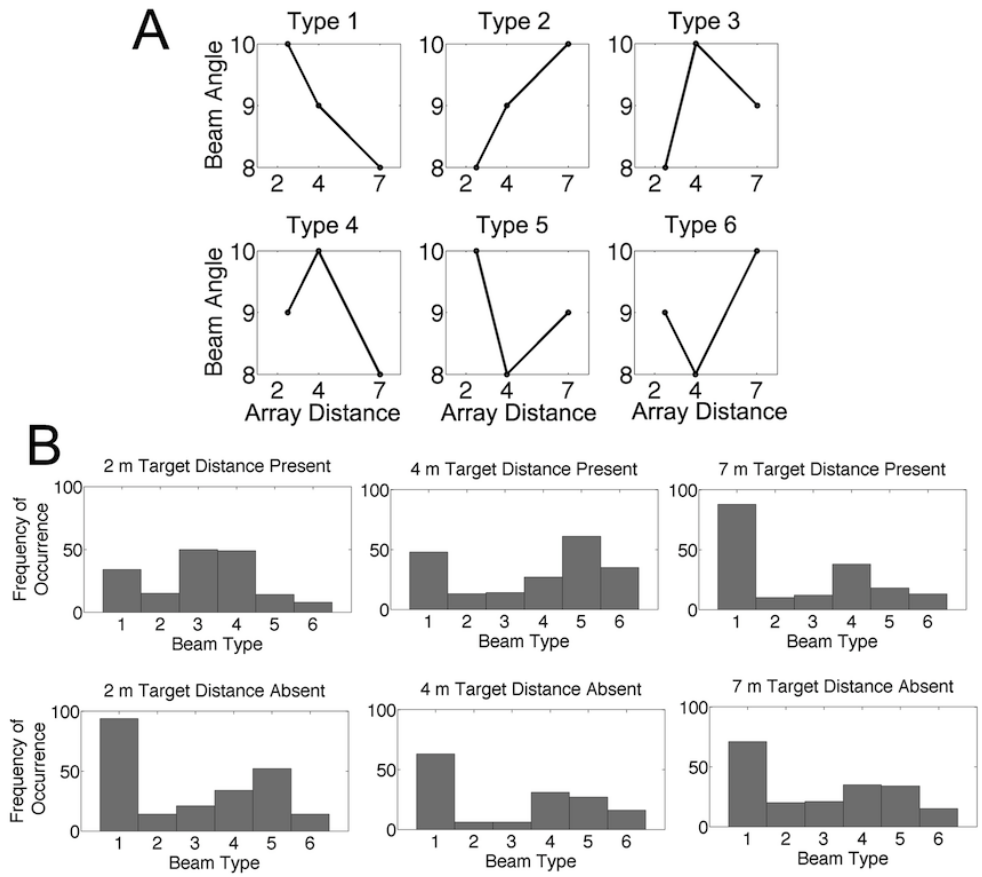

Figure 7: Distribution of differential beam focusing depending on target distance. a) Beams were classified by type according to the size of beam angle in degrees (see text). Numbers for beam angle on y-axis are not actual measurements, but rather examples for illustrative purposes. b) Frequency of occurrence of beam type depending on target distance and condition. If the whale were using an unfocused beam, we would expect an equal distribution of all beam types. If the whale were using a strategy of consistently narrowing the beam, we would expect Type 1 beams regardless of target distance. The differential distribution of beam types for the target present distances supports the hypothesis that the whale is focusing her beam onto the target at a given distance.

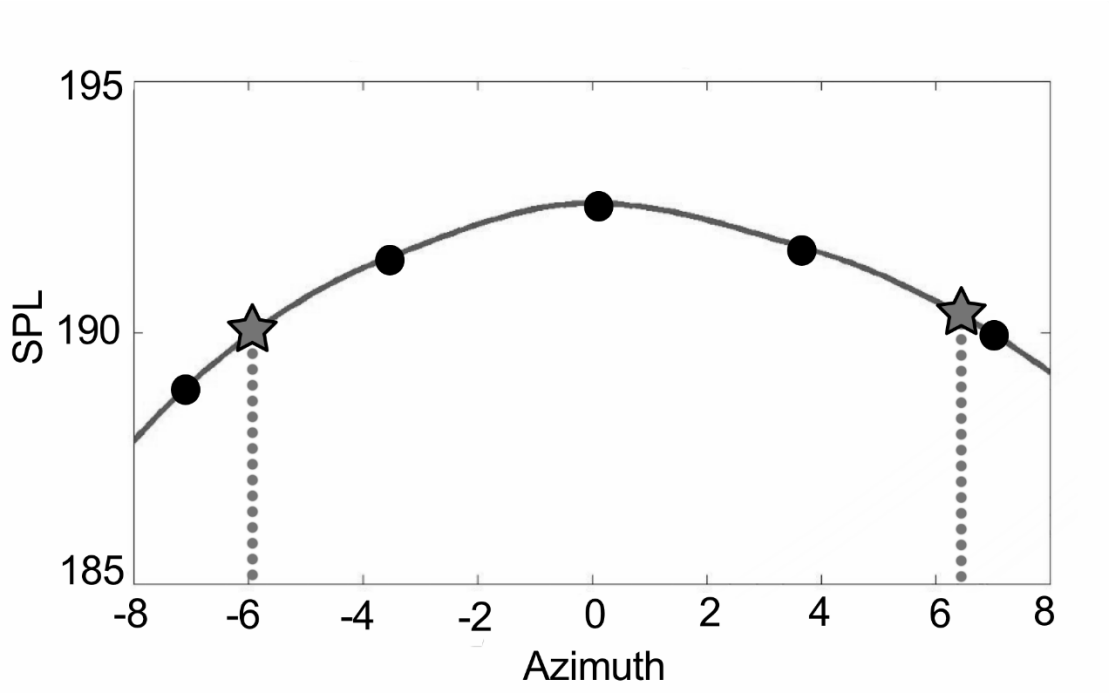

Fig. S1: Example of cubic interpolation and -3dB beamwidth calculation from a single echolocation click recorded on one linear array. Black circles indicate measured voltage values, converted to SPL (in dB re: 1µPa). Gray solid line indicates the results of cubic interpolation across all azimuth values (in degrees). Gray stars represent the SPL values that are 3 dB lower, or -3dB relative to, the peak recorded amplitude. Gray dotted line indicates the corresponding azimuth value for each -3dB value. The resulting -3dB beamwidth is calculated as the difference between the azimuthal values for each -3dB cutoff.